

Research Article

Modeling and Invulnerability Analysis of Multilayer Air Traffic Network considering Altitude Layer

Guangjian Ren  and Yin Liu

School of Traffic and Transportation, Beijing Jiaotong University, Beijing 100044, China

Correspondence should be addressed to Guangjian Ren; zc416418@126.com

Received 3 March 2023; Revised 9 May 2023; Accepted 2 June 2023; Published 16 June 2023

Academic Editor: Jiaqiang E

Copyright © 2023 Guangjian Ren and Yin Liu. This is an open access article distributed under the Creative Commons Attribution License, which permits unrestricted use, distribution, and reproduction in any medium, provided the original work is properly cited.

In this paper, a network coupling mechanism is studied to couple the air sector network, airport network, and air route network into a multilayer air network model. Then, the altitude layers are divided into three: high, medium, and low, and the arrival and departure flight procedures are also considered. By defining the association between the altitude layers and the waypoints, a multilayer air network model considering the altitude layer is constructed. Then, the line graph theory is used to redefine the nodes and edges, and the network is reconstructed to obtain a new single-layer one which is easy to calculate. Finally, a case study is carried out in Chengdu control area. The results show that the proposed model is closer to the reality, and the invulnerability performance is more referential. Besides, it also reflects the impact of altitude layers on the efficiency of airspace. The results are helpful for air traffic controllers to manage airspace better and have significance for promoting air traffic safety and stability.

1. Introduction

The whole process of flight refers to the aircraft that starts from the takeoff airport, flies along the specified air route (path) in airspace, and lands at the destination airport. In order to reduce the working pressure of controllers and improve the efficiency of the flight, the airspace is divided into several air sectors. In addition, the running range of aircraft is a three-dimensional space, which is the sector. Namely, the division of altitude layer (AL) is based on sector and air route. When an aircraft flies in air sectors, it uses different ALs, and the corresponding air routes are also distributed at different layers of altitude. Therefore, it is of practical significance to study the effect of the AL on the multilayer air network (MAN) and explore the influence of the ALs on the invulnerability, so as to improve the safety and reliability of air transport.

As is well known, flights have altitude restrictions when flying on the air route. According to statistics, the cruise altitude of flight is generally between 8000 meters and 12000

meters. Besides, the civil aviation department has set altitude restrictions on each air route in the airspace (such as one layer per 300 meters). Therefore, the altitude layer has a significant impact on the safety and reliability of flights. In addition, the utilization and operational efficiency of airspace are also limited by altitude layers. Constructing a MAN model considering the altitude layer is conducive to quantifying the impact of the altitude layers on the air traffic network. Simultaneously, it also simplifies the complexity of the influence of the altitude layer on the airspace. The proposed model provides a theoretical reference for reducing the load of air traffic controllers and improving the smoothness and safety of airspace. This is also one of the important contents of air traffic management.

The analysis of the characteristics of air transport network has attracted wide attention from scholars. As early as the past few years, some scholars have analyzed the aviation network of different countries, such as the weighted network of airports in India [1], the airline network in the United States [2], the air transport network in Europe [3],

and the Chinese airport network [4]. Zeng et al. [5] study the Chinese airline network structure based on complex network theory. In addition, scholars have also compared and analyzed the characteristics of aviation networks in different countries [6]. Wang et al. [7] analyze the network structure and nodal centrality of individual cities in the air transport network of China by a complex network approach. Besides, the structural similarity of air route systems in 58 countries is also studied [8]. Lin and Ban [9] analyze the features of American airline network over a 20-year period (1990-2010). The air traffic situation network [10], the international air transportation country network [11], and the Brazilian air transportation network [12] have also received the attention of the researchers. Then, the structure of Southeast Asian air transport network during 1979–2012 is analyzed [13]. Wang et al. [14] establish the world air sector network and analyze the topological characteristic.

In addition, the robustness or vulnerability of the aviation network is also the focus of the research. Clark et al. [15] discuss the robustness of the U.S. national airspace system airport network (NASAN). Moreover, the robustness of the global air transport network [16] and the European air traffic network [17] has also been studied. Then, Zanin et al. [18] analyze several typical transportation networks such as airport network, subway network, and bus network. In recent years, community structures in American airlines [19], robustness of weighted air transport networks (ATNs) [20], and resilience of the air traffic control sector network [21] have been studied by scholars. The robustness of Chinese air transport network during 1975-2017 is discussed by Chen [22]. Besides, the robustness of U.S. domestic air transportation from 2001 to 2016 has also been studied [23]. Zhang et al. [24] discuss the robustness of air transport network by weighted and unweighted approaches. Else, the robustness of air route network is analyzed via topology potential and relative entropy methods [25].

The structure of multilayer networks is also evolving in the study of transportation networks. For the European air transport network, Cardillo et al. [26] establish a multilayer network model and analyze its resilience. The world airline network is divided into three parts (core, bridge, and periphery), and then, the authors reveal its structural characteristics [27]. Similarly, the Chinese airline network is also analyzed as multilayer networks [28]. Hong et al. [29] investigate the structural properties of the Chinese air transport multilayer network, and the results highlight a better understanding of the Chinese air transport network. Moreover, Lordan and Sallan [30] study the multilayered structure of the European airport network (EAN). From a multilayered network, Zhang et al. [31] draw the topological properties of air transport network. In recent years, multilayer network theory is still applied to traffic networks, such as Chinese railway network [32], Chinese air transport network [33], the Southeast air transport system (United States) [34], and Chinese high-speed railway system [35].

From the above, previous studies rarely considered the impact of AL on air transport. In this paper, the impact of the AL on the stability of air transport network will be analyzed.

The rest of the paper is organized as follows: Section 2 is the model construction. Section 3 introduces the invulnerability of the model; the case analysis is in Section 4. Finally, Section 5 is the conclusion.

2. Model Construction

One of the main purposes of air traffic control service is to prevent aircraft from conflicts or even collisions in the air. When a sector is busy, it is necessary to ensure a sufficient safe distance between any two aircraft to prevent dangerous proximity between them. When aircraft are running along the air route, their speeds and headings may be different. Meanwhile, in order to ensure safety, they operate at different ALs. Generally, in order to improve the utilization efficiency of airspace, aircraft follow the principle of “east single and west double” in the flight level when flying on the air route (taking China as an example). The aircraft flying east can only choose odd ALs, and the aircraft flying west can only choose even ones, to ensure that there is at least one vertical separation between aircraft with different magnetic tracks. When the aircraft is at the same AL, it will fly according to the one-way rules.

2.1. Air Route Network. An air route is an air channel with a certain width, which presets the flight track of the aircraft. There are many kinds of structures in the air route. This section takes the crossing structure as an example to illustrate the altitude conversion of the aircraft. The crossing structure is shown in Figure 1(a). In the actual flight, it often occurs that the aircraft flying at the same altitude is in the same crossing route. Due to the incompressibility of the air route network (ARN), the aircraft cannot stop and wait, so the controllers generally adjust the altitude of the aircraft to ensure that there is sufficient interval between the encountering aircraft. Aircraft A1 and A2 are flying along different air routes at the same altitude. When the two air routes are about to cross, the aircraft A1 descends one altitude layer (AL) and the A2 rises another one, avoiding the occurrence of conflicts (see Figure 1(b)).

Besides cross encounters, aircraft often need to change the AL to ensure flight safety when flying in the air route. Therefore, when analyzing the structural performance of the ARN, it is necessary to consider the influence of AL on the actual flight and build a multilayer network model.

In this section, based on the analysis of network topology and properties, the cruise altitude range of aircraft is divided into three layers: lower (L_L), moderate (L_M), and higher (L_H), and it is assumed that the three layers have the same direction. Therefore, when considering the AL to construct a new ARN, there will be a three-edge connection between two waypoints; that is, all three types of ALs can connect waypoints, as shown in Figure 2.

In an undirected graph, if there is more than one connection between two nodes, a multiple graph is obtained. The ARN considering the AL is a multigraph, and different ALs on the same air route are the parallel edges of the multigraph. The ARN based on the AL is $G_C = \{U_C, E_C\}$, where $U_C = \{u_{i,C} \mid i = 1, 2, \dots, n_C\}$ is the set of waypoints and

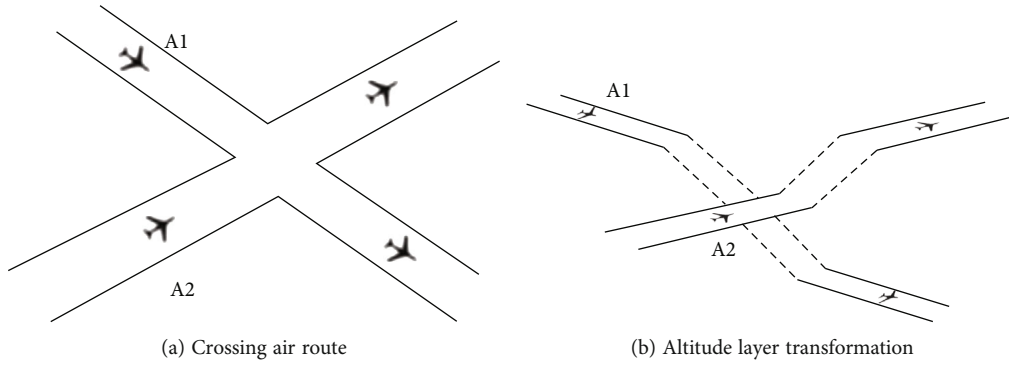


FIGURE 1: Diagram of crossing air route.

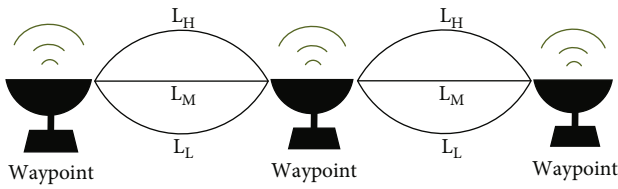


FIGURE 2: Air route network with altitude layers.

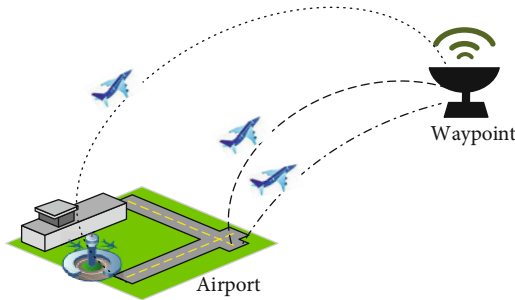


FIGURE 3: The approach and departure flight procedure of the airport.

$E_C = \{e_C^{ij} = (u_{i,C}, u_{j,C}) \mid i = 1, 2, \dots, n_C; j = 1, 2, \dots, n_C; i \neq j\}$ is the set of edges. The edge of the ARN can be obtained as

$$e_C^{ij} = \begin{cases} k, & k \text{ connected altitude layers between waypoints } u_i \text{ and } u_j, \\ 0, & \text{no connection between waypoints } u_i \text{ and } u_j, \end{cases} \quad (1)$$

where k is the multiplicity of edge e_{ij} , $k = 3$.

2.2. Airport Network Model. The flight process includes take-off and departure, cruise, approach, and landing. Generally, airport runways are available in two directions for aircraft to take off or land. Some airports have two or more runways, and all airports generally have multiple flight procedures for arrival and departure. In this case, there should be multiple connections between the nodes of airport network (AIN) and air route network (ARN) (see Figure 3).

In this section, assume that each airport has three sets of two-way arrival and departure flight procedures. Consider the flight procedure factors to analyze the coupling mechanism between the two networks. The connection relationship between AIN nodes and ARN nodes is expressed in

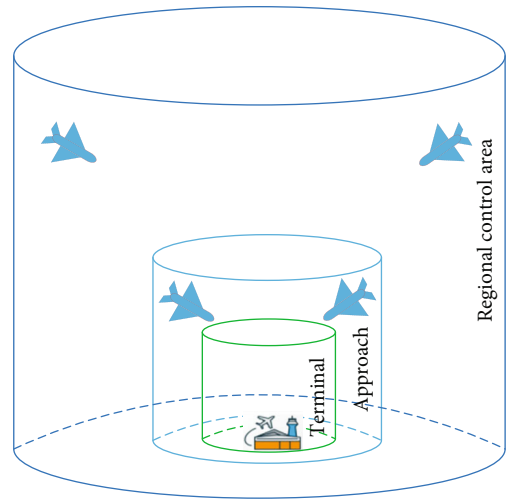


FIGURE 4: Diagram of airspace classification.

the form of adjacency matrix. Then, the element e_{BC}^{ij} of adjacency matrix E_{BC} between AIN (G_B) and ARN (G_C) is

$$e_{BC}^{ij} = \begin{cases} k, & k \text{ flight procedures between airport } u_{i,B} \text{ and waypoint } u_{j,C}, \\ 0, & \text{airport } u_{i,B} \text{ does not pass waypoint } u_{j,C}, \end{cases} \quad (2)$$

where k is the multiplicity of edge e_{BC}^{ij} , $k = 3$.

2.3. Air Sector Network. In China, the airspace is divided into regional control area, approach area, and terminal (tower) area, as shown in Figure 4.

As shown in Figure 4, the terminal area corresponds to the tower control airspace, the approach area corresponds to the approach control airspace, and the regional control area corresponds to the middle, the low, and the high altitude control airspace. When constructing the air sector network (ASN) model, the high altitude control airspace is taken as an example, and its air sector is the node.

On the other hand, the air sector is an abstract concept defined artificially. Its role is mainly reflected in the control process of the ARN and the AIN. The air sector is regarded as a node, so that the airports and waypoints in the air sector are connected to the ASN nodes. If one air sector is closed,

all waypoints in the air sector will be failure and the ALs will also be closed. In order to make the new model closer to the actual flight of the aircraft along the air route, the influence of the air sector on the AL of the air route is reflected in the failure of the edge. Thus, the ASN (G_A) model is constructed. In essence, the topology of ASN is consistent without considering the ALs.

2.4. Multilayer Air Network Model. In this section, altitude layers of lower, moderate, and higher in the same direction are taken as the edges of the ARN. Besides, multiple arrival and departure flight procedures are also taken to represent the multilayer air network (MAN) model between ARN and AIN. The topology of the MAN model is restored graphically, as shown in Figure 5.

Figure 5 is the MAN model considering the ALs, in which the blue solid line; the red solid line and the green solid line represent the inner edge of the ASN, the ARN, and the AIN, respectively. The red-dotted lines represent the added AL connection, and the yellow-dotted lines represent the added flight procedure connection.

In short, the MAN is a multilayer coupled network that mainly includes airport network (AIN), air sector network (ASN), and air route network (ARN). Besides, ASN and ARN consider the influence of the altitude layers and divide the altitude layers into three categories: high, medium, and low. Meanwhile, the AIN considers the arrival and departure flight procedures.

2.5. Network Reconstruction Analysis. In the above, the MAN model is constructed by considering the AL, which simulates the failure of a certain route in the ARN or the failure of a certain AL, that is, the attack on the edge of the ARN. Therefore, we consider expanding the coverage of ARN (considering the approach and departure procedures) and improving the degree of coverage of the flight process of the aircraft.

Airport terminal areas are generally equipped with Instrument Landing Systems (ILS), including distance, direction guidance, and visual reference systems to guide aircraft during landing.

Therefore, the airport has standard navigation facilities, which can be regarded as a waypoint in the ARN. The departure stage and the approach stage can be regarded as the flight segment (because the departure stage and the approach stage together form the process of landing at the airport after leaving the air route, this paper regards the two stages as one flight segment). Furthermore, the airport is regarded as a waypoint, and the outer link between ARN and AIN representing the arrival and departure procedures is regarded as an edge in the ARN. The AIN is integrated into the ARN, thus covering the whole flight process of the aircraft more completely.

The integrated ARN (including airport nodes and arrival and departure procedures links) has the topological characteristics shown in Figure 2; that is, there are multiple connections between two waypoints. When an edge of the ARN is attacked, the failure principle is as follows: when an edge of the network is attacked, only the edge fails, and there is still a link between the two waypoints because there are other edges between the waypoints. When all the edges

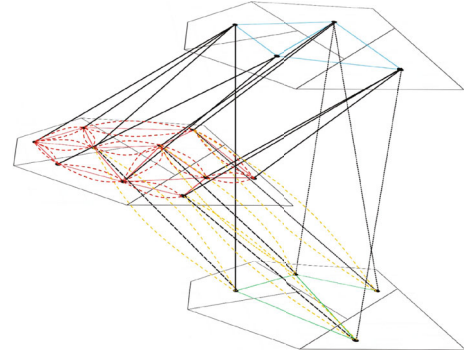


FIGURE 5: The multilayer air network model.

between two waypoints fail, the two waypoints will disconnect. Therefore, it is necessary to make node-edge transformation for the ARN, which can help to analyze the influence of the AL on the MAN model.

Line graph theory has played a role in the study of complex networks. In this theory, the topological relationship between edges is considered, and edges are regarded as node sets.

In this section, the edge of the original MAN is regarded as the node of a new network by using the line graph theory. If two edges of the original MAN have common nodes, a new edge is formed between the new nodes (transformed from the two original edges), and a new coupling network is constructed. This coupling network emphasizes the topological connection between the edges of the original MAN. For example, Figure 6(a) is a network with five edges, whose edges A, B, C, D, and E are transformed into nodes A, B, C, D, and E in the new network, respectively. Taking edge A as an example, it converges on one node with edges C, D, and E in the original network, so node A connects C, D, and E when transformed into a new network. After analyzing five edges in turn, a new network is formed, as shown in Figure 6(b).

The adjacency matrix of the network can represent the connection relationship between nodes in the network, but it cannot directly reflect the relationship between nodes and edges. In order to transform the network, it is necessary to obtain the connection relationship between nodes and edges in order to further obtain the relationship between edges. Here, another method of representing the network is introduced, namely, the incidence matrix.

Let G be a network with n nodes and m edges; then, its incidence matrix is $B = (b_{ij})_{n \times m}$, whose elements are

$$b_{ij} = \begin{cases} 1, & \text{Edge } j \text{ passes through node } i, \\ 0, & \text{Edge } j \text{ does not pass through node } i. \end{cases} \quad (3)$$

The incidence matrix represents the relationship between nodes and edges in the network. The transformed network of G is denoted as L_G , and the adjacency matrix of L_G can be further obtained by the incidence matrix of G , which is expressed as

$$A(L_G) = B^T B - 2I_m, \quad (4)$$

where I_m is the unit matrix of order m .

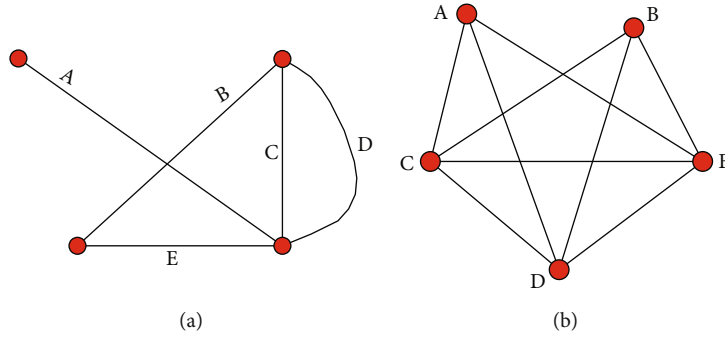


FIGURE 6: Node-edge transformation of networks.

3. Invulnerability Analysis

In general, the air traffic network operates normally according to the established functions. However, when some structures of the network are damaged, the failure of nodes or edges will directly lead to the destruction of the functions of the network. When the network is damaged, the network structure function changes but still can maintain normal operation, indicating that the network has better invulnerability. Since various types of networks have different characteristics, the invulnerability needs to be defined according to the specific system or network studied.

3.1. Invulnerability of the Multilayer Air Network. The MAN model is a coupled and interconnected multilayer network. When the performance of nodes or edges in the network decreases or even fails due to destructive events, this effect will spread rapidly through the connection relationship between multilayer networks and eventually cause the failure of local or even the whole network. In this section, the invulnerability of MAN is defined as the ability to maintain basic connectivity and complete normal operation after the network is damaged.

In the process of invulnerability analysis of MAN, the method of attacking nodes can be used to simulate the actual destructive events. The attack methods are divided into random attack and deliberate attack. Random attack is to delete nodes with the same probability in the network. Deliberate attack is to rank the nodes according to the degree and then delete the nodes from high to low according to the degree value. When the node degree value is the same, it is deleted according to the equal probability.

3.2. Invulnerability Analysis Indicators. When the MAN is attacked, the size of the network and the shortest path length will change significantly. This section analyzes the network invulnerability by using size of the giant component and the network efficiency.

3.2.1. Network Efficiency. Network efficiency is the reciprocal of the average shortest path length of the network, which is mainly used to show the overall efficiency of the network and the degree of connectivity between nodes. Its expression is

$$E = \frac{2}{N(N-1)} \sum_{i \neq j \in G} \frac{1}{d_{ij}}, \quad (5)$$

where E is the network efficiency, $0 < E < 1$, in which the greater the value, the higher the network transportation efficiency, $E = 1$, the nodes in the network are all connected, N is the total number of nodes, and d_{ij} is the shortest path length between nodes i and j in the MAN. If there is no connected path between nodes i and j , d_{ij} tends to infinity, $1/d_{ij} = 0$.

3.2.2. Size of the Giant Component. After the network is destroyed, the subgraph containing the most nodes in the network and paths between any nodes is defined as the giant component. In the MAN, the size of the giant component can describe the size of the remaining one that can still operate normally after being attacked. In this section, the relative size S of the giant component will be used to represent the invulnerability. S represents the ratio of the number of nodes in the giant component after the MAN is attacked to the total number of nodes before the attack. The formula is as follows:

$$S = \frac{N'}{N}, \quad (6)$$

where N is the total number of nodes and N' is the number of nodes in the giant component. It is obvious that the larger the S ($0 < S < 1$) is, the higher the integrity of MAN is. In the initial MAN, $S = 1$.

4. Case Analysis

4.1. Data. In this paper, taking the data of Chengdu control area (CCA) in China as an example, the model of CCA is obtained by adjacency matrix. In CCA, the ASN contains 7 nodes and 10 edges, the AIN contains 10 nodes and 15 edges, and the ARN contains 52 nodes and 82 edges. The basic structure of CCA is shown in Figure 7, where black points represent the nodes and red solid lines represent the edges.

Based on the complex network theory, the three networks contained in the CCA are analyzed, and the basic parameters are shown in Table 1.

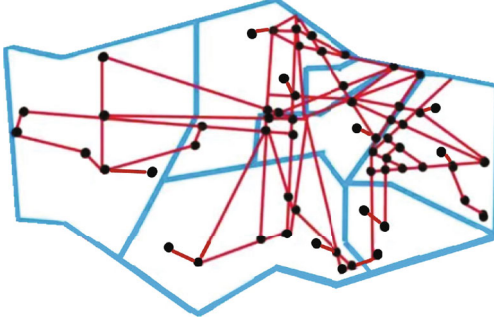


FIGURE 7: Diagram of the CCA.

TABLE 1: Basic parameter values of CCA.

Parameter	ASN (G_A)	AIN (G_B)	ARN (G_C)
Nodes	7	10	52
Edges	10	15	82
Average path length	1.619	1.800	6.002
Degree-degree relativity	-0.250	-0.664	0.115

Table 1 shows that when a flight is flying in the CCA, it needs to pass through two air sectors on average; that is, it is under the command of two sectors. On average, 2 flights are required to connect any two airports in CCA. When flying in CCA, the flight needs to pass through 6 important waypoints on average. In addition, the ARN is positively correlated, that is, assortative, and the ASN and the AIN are negatively correlated, that is, disassortative. Among the three networks, only the AIN has significant disassortativity. This is in line with the law of air transport: airports with fewer airlines (nodes with smaller degrees) tend to be connected to airports with more airlines (nodes with larger degrees), while nodes in the ARN or nodes in the ASN are generally connected to neighboring ones.

4.2. The Multilayer Network Model of Chengdu Control Area.

According to the connection relationship within the three networks of the CCA and the coupling relationship among them, if there is an edge between the nodes, the corresponding matrix element is "1," and the adjacency matrix is established. Based on the coupling mechanism of multilayer network, its topology is shown in Figure 8.

As shown in Figure 8, let $g = \{G_A, G_B, G_C\}$ be a set of three networks, where G_A , G_B , and G_C represent the ASN, AIN, and ARN, respectively. The connection between the three networks is the outer edge $e = \{E_{AB}, E_{AC}, E_{BC}\}$, where E_{AB} represents the influence between ASN and AIN and E_{AC} or E_{BC} have similar meanings. Thus, the multilayer network of CCA is $G_M = \{g, e\}$.

Then, according to the characteristics of the AL, the G_M in CCA is reconstructed, and the MAN (G_p) considering the AL is obtained. Its topology is shown in Figure 9.

As shown in Figure 9, the MAN has 69 nodes and 348 edges, where the red-dotted lines represent the added edges of ALs and flight procedures. In order to facilitate the invul-

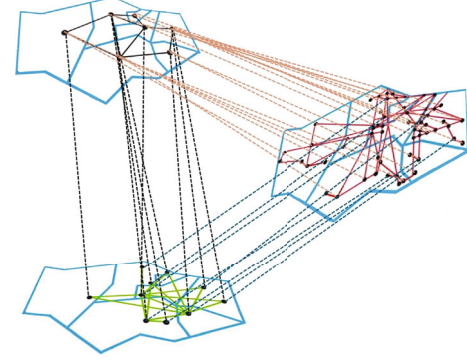


FIGURE 8: The multilayer network of CCA.

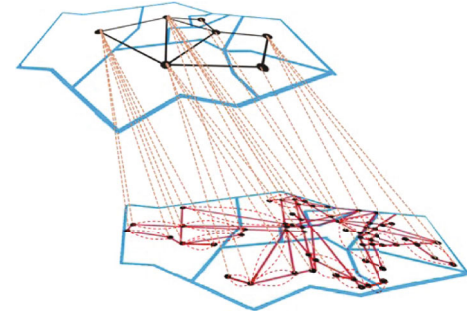
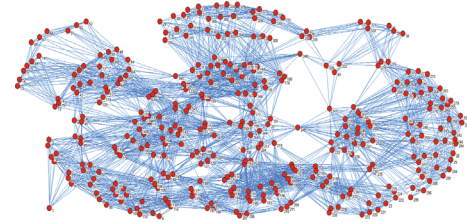


FIGURE 9: The MAN model considering altitude layer in CCA.

FIGURE 10: Composite network G_Q of CCA.

nerability analysis of the MAN, the line graph theory is used to transform the MAN (G_p).

Let G_p be transformed into a composite network G_Q , and the incidence matrix $B(G_p)$ of G_p is obtained according to Equation (3). Based on Equation (4), combining $B(G_p)$ and the transposed matrix $B(G_p)^T$, the connection relation of nodes in G_Q can be obtained. Finally, the adjacency matrix $A(G_Q)$ is obtained, and the topology of G_Q can be obtained as shown in Figure 10.

4.3. *Invulnerability Analysis.* According to the actual flight of air transport, when the air sectors, airports, and waypoints are closed, it will not cause the adjacent ones to be closed, which is reflected in the MAN; that is, the failure of nodes in the subnet will not lead to the failure of other nodes in the same subnet. In addition, when the air sector is closed, it will affect the waypoints and airports in the sector; namely, its internal airports or waypoints will be closed. Therefore, the impact of single-layer network failure on other ones is as follows:

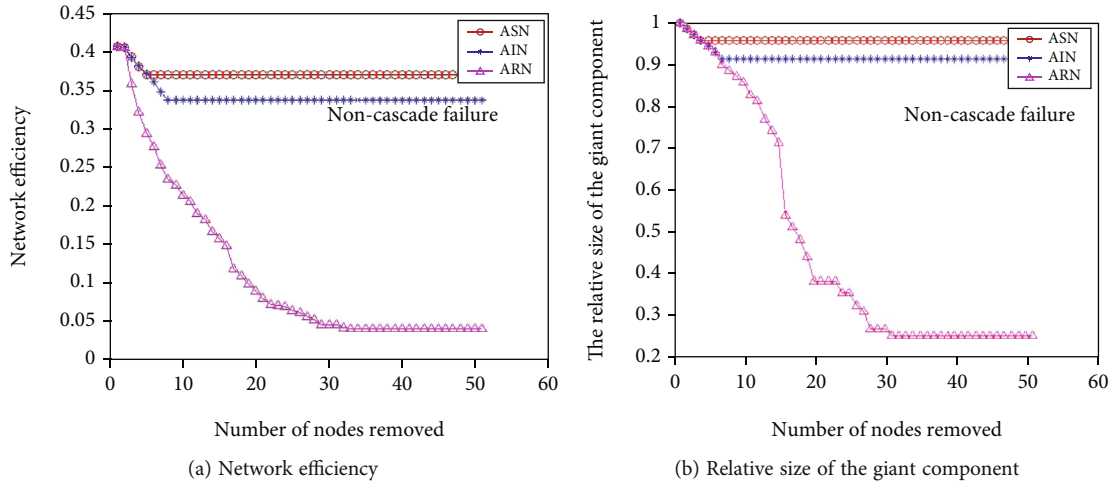


FIGURE 11: Invulnerability of MAN under noncascading failure.

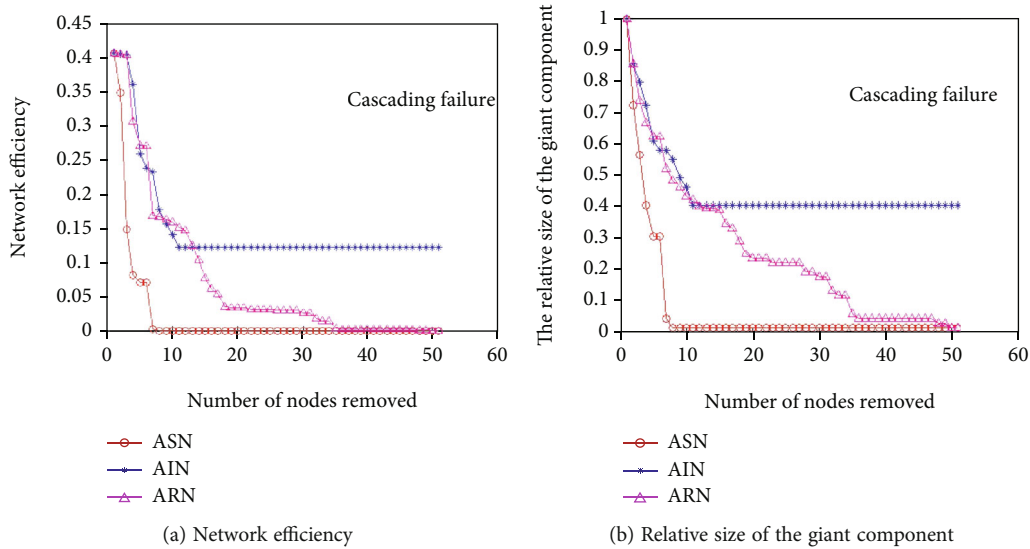


FIGURE 12: Invulnerability of MAN under cascading failure.

4.3.1. *Failure of Air Sector Network.* When one air sector is closed for some reason, the sector node fails, and the edge connecting the sector fails immediately. The airports and waypoints within the control scope of the sector also fail.

4.3.2. *Failure of Airport Network.* When the airport cannot be used for some reason, the node fails, the connected edge immediately fails, and the waypoints and air sectors connected to it do not fail.

4.3.3. *Failure of Air Route Network.* When the waypoint is unable to be used for some reason, the node fails, and the edge connected to the waypoint immediately fails. If all aircraft of the airport enter the air route through the waypoint, the airport shall fail. In contrast, if the aircraft of the airport can also enter the air route through other waypoints, the airport does not fail. The sectors connected to the failed waypoints still operate normally, so the air sector does not fail.

(1) *Invulnerability of G_M .* According to the characteristics of MAN in CCA, the invulnerability of the network is analyzed from two aspects: (a) noncascading failure, that is, there is no coupling relationship between different networks, and (b) cascading failure, that is, there is a coupling relationship between the networks. Then, the nodes in the ASN (G_A), AIN (G_B), and ARN (G_C) are attacked from large to small according to the degree value. The relative size of the giant component and the network efficiency of the MAN is counted, and the influence of the three networks on the MAN is analyzed.

From the results of Figures 11 and 12, it can be seen that, on the whole, the ARN has the greatest impact on the entire MAN, which can lead to the almost total loss of operation function of the MAN. In the case of noncascade failure, the influence of the AIN and the ASN on the entire MAN is relatively close. Finally, the relative size of the giant component and the network efficiency is stable at similar values,

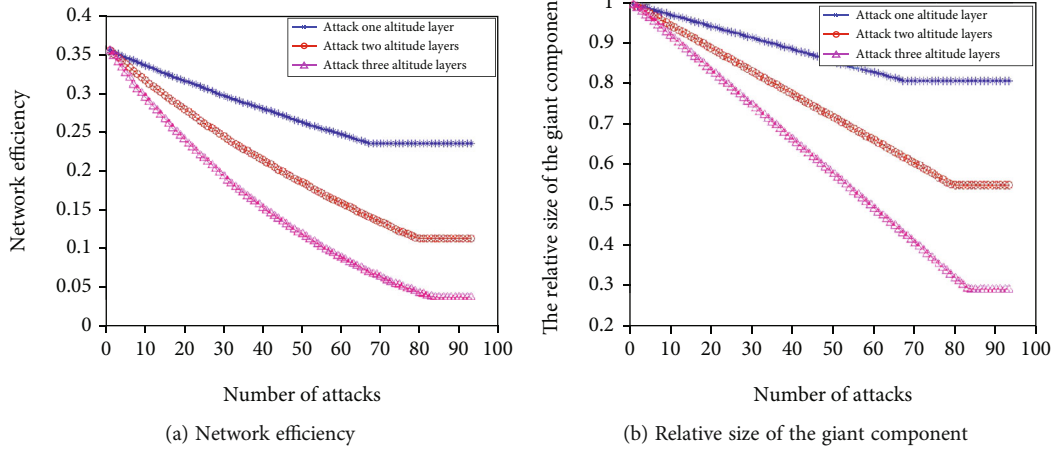


FIGURE 13: Invulnerability effect of altitude layer on the MAN.

and the MAN can still maintain normal operation to a certain extent. However, in the case of cascading failure, airspace (sector) has the greatest impact on the invulnerability of MAN, and its reliability plays a central role in the stability of air traffic. In summary, ARN and ASN have the greatest impact on the integrity of MAN. Therefore, in order to ensure the safety and reliability of air traffic, the stability and integrity of ARN and ASN should be guaranteed. Simultaneously, this provides a theoretical reference for the air traffic control service, which is conducive to the air traffic control department to formulate accurate and effective strategies.

(2) *Invulnerability of G_p* . In the network G_p , the same segment contains three ALs. In this experiment, the three ALs are transformed into nodes and their degrees are equal. In order to compare and analyze the influence of ALs on the MAN, the following attack experiments are carried out:

- (a) One of the ALs of all air routes is selected, and the deliberate attack is carried out according to the degree from large to small. In this case, the air routes remain connected
- (b) Pick out two ALs of the same air route from ARN, and carry out deliberate attacks from large to small according to the degree. In this case, the air routes also remain connected
- (c) Select all of the ALs of the ARN, and carry out deliberate attacks from large to small according to the degree. In this case, the air routes will be disconnected

The invulnerability of the G_p under three attack cases is shown in Figure 13.

From Figure 13, the ALs of the same air route are similar in characteristics, so the variation of both network efficiency and size of the giant component tends to be proportional on the whole. The attack on one AL of the

TABLE 2: Number of nodes of the giant component under attack.

Number of attacks	Number of failed nodes	Size of the giant component
1	1	348
2	2	347
3	3	346
4	4	345
5	5	344
6	6	343
7	7	342
8	8	341
9	9	340

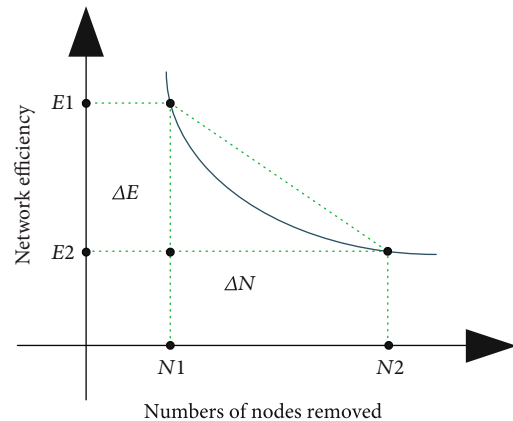


FIGURE 14: The change of network efficiency.

air route has little effect on the MAN. The network efficiency changes by about 25%, and the relative size of the giant component changes by about 20%. However, when the three ALs of the air routes are attacked, the MAN is greatly affected, and network efficiency and size of the giant component can change by about 70%. Therefore, the

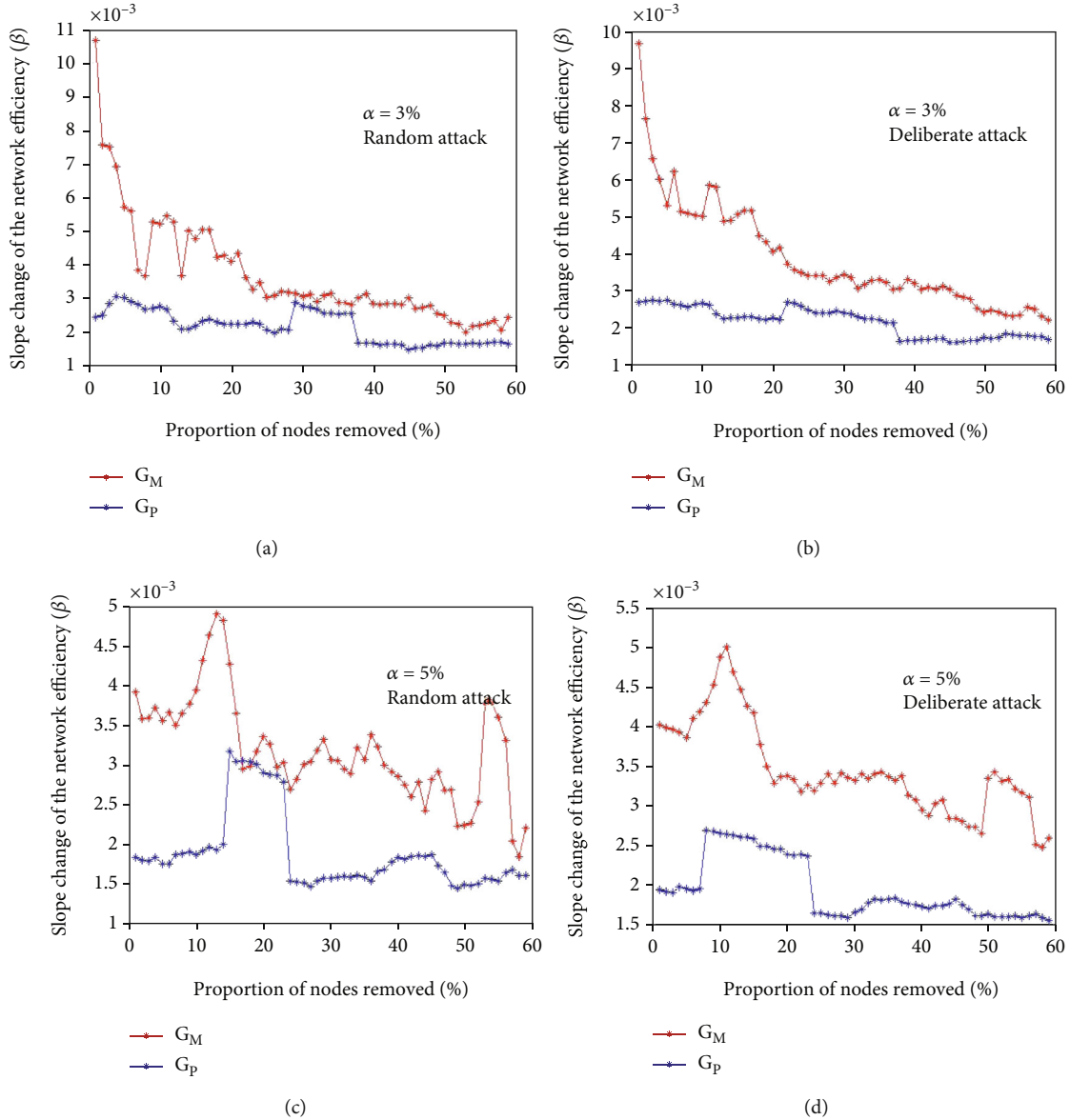


FIGURE 15: Comparison of invulnerability between G_P and G_M .

addition of the AL enhances the invulnerability of MAN to a certain extent, so that it can resist external interference better.

(3) Comparative Analysis of Invulnerability between G_M and G_P .

(a) Indicator selection

The three ALs of the same air route are connected to the same waypoints, so when the ALs are regarded as nodes, the nodes have the same degree; that is, the network G_P has certain aggregation and regularity. Meanwhile, when network G_P is attacked, the size of the giant component changes regularly, and its change rule is shown in Table 2.

It can be seen from Table 2 that the size of the giant component decreases regularly when the network G_P is attacked, and it has no reference value in the comparative

analysis of invulnerability between G_M and G_P . Therefore, in this section, the network efficiency is mainly used as the research indicator. By comparing the relative changes of the network efficiency both G_M and G_P , the invulnerability characteristics of G_M and G_P are studied.

From Section 5, the network efficiency is expressed as

$$E = \frac{2}{N(N-1)} \sum_{i \neq j \in G} \frac{1}{d_{ij}}, \quad (7)$$

where E is the network efficiency and N is the total number of nodes.

Thus, the curve of network efficiency E with N is obtained (see Figure 14).

Figure 14 is an example of the change in network efficiency after the network is attacked, where the proportion of nodes attacked is α and the slope change of the network efficiency is

$$\beta = \frac{E_1 - E_2}{N_1 - N_2} = \frac{\Delta E}{\Delta N} = \frac{\Delta E}{\alpha N}, \quad (8)$$

where the slope change of network efficiency is β , ΔE is the relative change of network efficiency, and ΔN is the relative change of nodes. The larger the β , the faster the network efficiency E changes, and the greater the impact on invulnerability.

In addition, the relative entropy theory (RET) is introduced to improve the accuracy of invulnerability analysis. RET can represent the information difference between vectors $A(x)$ and $B(x)$, and its expression ($K(A||B)$) is

$$K(A||B) = \sum A(x) \log \frac{A(x)}{B(x)}. \quad (9)$$

The greater the relative entropy ($K(A||B)$), the greater the difference between the two vectors $A(x)$ and $B(x)$, that is, the more serious the element changes. Thus, if K_β represents the relative entropy with $\beta \in (0, 1]$, then

$$K_\beta = \frac{\beta}{\beta_{\max}} \log \frac{\beta/\beta_{\max}}{\beta'/\beta_{\max}} + \left[1 - \frac{\beta}{\beta_{\max}}\right] \log \left(\frac{1 - (\beta/\beta_{\max})}{1 - (\beta'/\beta_{\max})} \right), \quad (10)$$

where β is the slope of the original air traffic network efficiency and β' is the slope of the network efficiency after the AL closure. β_{\max} and β'_{\max} are the maximum values, and $\beta_{\max} = \beta'_{\max} = 1$. Therefore,

$$K_\beta = \beta \log \frac{\beta}{\beta'} + [1 - \beta] \log \left(\frac{1 - \beta}{1 - \beta'} \right). \quad (11)$$

Normally, $\beta = [\beta_1, \beta_2, \dots, \beta_n]$ is a vector with n elements, and its mean value $\bar{\beta}$ is

$$\bar{\beta} = \frac{1}{n} \sum_{i=1}^n \beta_i. \quad (12)$$

Then, after the i ALs of the MAN are closed, the relative entropy of $\bar{\beta}_i$ is expressed as

$$\bar{K}_{\bar{\beta}_i} = \bar{\beta} \log \frac{\bar{\beta}}{\beta_i} + [1 - \bar{\beta}] \log \left(\frac{1 - \bar{\beta}}{1 - \beta_i} \right), \quad (13)$$

where $\bar{K}_{\bar{\beta}_i}$ represents the relative entropy of $\bar{\beta}_i$ when $i \in [1, 2, 3]$ ALs cannot be used (closed), reflecting the

TABLE 3: Mean slope of network efficiency.

Indicators	$\bar{\beta}$	$\bar{\beta}_1$	$\bar{\beta}_2$	$\bar{\beta}_3$
Values	0.0020	0.0014	0.0028	0.0035

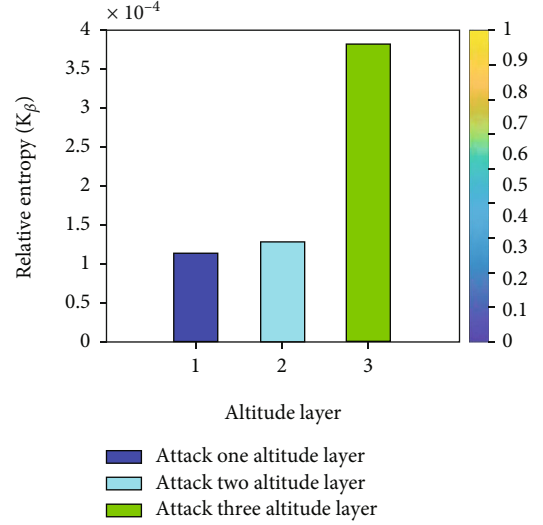


FIGURE 16: The relative entropy of $\bar{\beta}_i$.

speed of change in network efficiency. The larger the $\bar{K}_{\bar{\beta}_i}$, the weaker the vulnerability of MAN, and the more obvious the influence of external factors. Therefore, $\bar{K}_{\bar{\beta}_i}$ can show the impact of AL on the vulnerability of air traffic network objectively and accurately.

(b) Results analysis

Random attacks and deliberate attacks on both G_p and G_M are carried out to obtain their network efficiency. Then, the slope change of the network efficiency is obtained, under $\alpha = 3\%$ and $\alpha = 5\%$. The results are shown in Figure 15.

It can be clearly seen from Figure 15 that the slope change β of G_p is relatively stable and smaller than that of the G_M , which proves that the stability of G_p is relatively good. Meanwhile, when α changes from 3% to 5%, the slope change β of G_p has always been smaller than that of G_M and the gap has a tendency to expand. Therefore, network G_p by considering the ALs performs better than that of G_M in terms of invulnerability. Therefore, the coupling model G_p considering the ALs is closer to reality, and its structural performance is more referential for air traffic.

Further, when there is an attack from large to small by degree, the values of $\bar{\beta}$ and $\bar{\beta}_i$ can be obtained, as shown in Table 3.

According to Equation (13), the relative entropy results are shown in Figure 16.

It is clear from Figure 16 that $\bar{K}_{\bar{\beta}_3} > \bar{K}_{\bar{\beta}_2} > \bar{K}_{\bar{\beta}_1}$, which indicates that the vulnerability of the air traffic network is related to the ALs. The more available ALs, the stronger

the anti-interference ability of air traffic. With the decrease of available ALs, the operation ability of airspace is also affected. As a result, the airspace efficiency is reduced and the vulnerability of air traffic will become weaker. The results can provide reference for improving the ability of air traffic control (ATC). Providing more available ALs can improve airspace utilization effectively, thereby reducing air congestion. Moreover, it can also improve the punctuality rate of flights.

5. Conclusions

In this paper, the Chengdu control area (CCA) is taken as an example, and then, a MAN model considering ALs is constructed. The structural characteristics of MAN are analyzed, and the influences of ASN, AIN, and ARN on the structure of MAN are given. Next, the effect of AL on the invulnerability of MAN is discussed. Finally, combined with the slope change of network efficiency, the invulnerability performance between the MAN considering AL and the MAN without considering AL is compared. The results show that the invulnerability of the MAN model considering the AL is closer to the reality, and its performance data is more referential. At the same time, it can also improve the smoothness and efficiency of the airspace. Suggestions are as follows:

- (1) Reasonably delineate altitude layers based on the characteristics of the air routes
- (2) Develop reasonable measures to reduce the altitude separation between flights
- (3) When conducting air traffic control, the operation of main altitude layers in airspace shall be focused

In the future, other characteristics of airspace can be further analyzed to construct a more comprehensive MAN model, so as to provide a reliable reference for improving the efficiency of air traffic control.

Data Availability

The data used to support the findings of this study are available from the corresponding author upon request.

Conflicts of Interest

The authors declare that they have no conflicts of interest

Acknowledgments

This work is supported by the Fundamental Research Funds for the Central Universities (No. 2021RC214).

References

- [1] G. Bagler, "Analysis of the airport network of India as a complex weighted network," *Physica A*, vol. 387, no. 12, pp. 2972–2980, 2008.
- [2] Z. Xu and R. Harriss, "Exploring the structure of the U.S. inter-city passenger air transportation network: a weighted complex network approach," *GeoJournal*, vol. 73, no. 2, pp. 87–102, 2008.
- [3] D. D. Han, J. H. Qian, and J. G. Liu, "Network topology and correlation features affiliated with European airline companies," *Physica A*, vol. 388, no. 1, pp. 71–81, 2009.
- [4] J. Zhang, X. B. Cao, W. B. Du, and K. Q. Cai, "Evolution of Chinese airport network," *Physica A*, vol. 389, no. 18, pp. 3922–3931, 2010.
- [5] X. Z. Zeng, X. X. Tang, and K. S. Jiang, "Empirical study of Chinese airline network structure based on complex network theory," *Journal of Transportation Systems Engineering and Information*, vol. 11, no. 6, pp. 175–181, 2011.
- [6] S. Paleari, R. Redondi, and P. Malighetti, "A comparative study of airport connectivity in China, Europe and US: which network provides the best service to passengers?," *Transportation Research Part E*, vol. 46, no. 2, pp. 198–210, 2010.
- [7] J. Wang, H. H. Mo, F. H. Wang, and F. J. Jin, "Exploring the network structure and nodal centrality of China's air transport network: a complex network approach," *Journal of Transport Geography*, vol. 19, no. 4, pp. 712–721, 2011.
- [8] X. Sun and S. Wandelt, "Network similarity analysis of air navigation route systems," *Transportation Research Part E*, vol. 70, pp. 416–434, 2014.
- [9] Y. F. Lin and Y. F. Ban, "The evolving network structure of US airline system during 1990-2010," *Physica A: Statistical Mechanics and its Applications*, vol. 410, pp. 302–312, 2014.
- [10] H. Y. Wang, R. Y. Wen, and Y. F. Zhao, "Analysis of topological characteristics in air traffic situation networks," *Journal of Aerospace Engineering*, vol. 229, no. 13, pp. 2497–2505, 2015.
- [11] S. Wandelt and X. Q. Sun, "Evolution of the international air transportation country network from 2002 to 2013," *Transportation Research Part E*, vol. 82, pp. 55–78, 2015.
- [12] G. S. Couto, A. P. C. Da Silva, L. B. Ruiz, and F. Benevenuto, "Structural properties of the Brazilian air transportation network," *Anais da Academia Brasileira de Ciencias*, vol. 87, no. 3, pp. 1653–1674, 2015.
- [13] L. Dai, B. Derudder, and X. J. Liu, "The evolving structure of the Southeast Asian air transport network through the lens of complex networks, 1979-2012," *Journal of Transport Geography*, vol. 68, pp. 67–77, 2018.
- [14] Y. Wang, K. Meng, H. D. Wu, J. Hu, and P. Wu, "Critical airports of the world air sector network based on the centrality and entropy theory," *International Journal of Modern Physics B*, vol. 35, no. 6, article 2150081, 2021.
- [15] K. L. Clark, U. Bhatia, E. A. Kodra, and A. R. Ganguly, "Resilience of the U.S. national airspace system airport network," *IEEE Transactions on Intelligent Transportation Systems*, vol. 19, no. 12, pp. 3785–3794, 2018.
- [16] O. Lordan, J. M. Sallan, P. Simo, and D. Gonzalez-Prieto, "Robustness of the air transport network," *Transportation Research Part E*, vol. 68, pp. 155–163, 2014.
- [17] K. C. Pien, K. Han, W. L. Shang, A. Majumdar, and W. Ochieng, "Robustness analysis of the European air traffic network," *Transportmetrica A: Transport Science*, vol. 11, no. 9, pp. 772–792, 2015.
- [18] M. Zanin, X. Sun, and S. Wandelt, "Studying the topology of transportation systems through complex networks: handle with care," *Journal of Advanced Transportation*, vol. 2018, Article ID 3156137, 17 pages, 2018.

- [19] W. W. Wu, H. Y. Zhang, S. R. Zhang, and F. Witlox, "Community detection in airline networks: an empirical analysis of American vs. Southwest airlines," *Journal of Advanced Transportation*, vol. 2019, Article ID 3032015, 11 pages, 2019.
- [20] Y. Zhou, J. Wang, and G. Huang, "Efficiency and robustness of weighted air transport networks," *Transportation Research Part E*, vol. 122, pp. 14–26, 2019.
- [21] X. Wang, S. Miao, and J. Tang, "Vulnerability and resilience analysis of the air traffic control sector network in China," *Sustainability*, vol. 12, no. 9, p. 3749, 2020.
- [22] Y. Chen, J. Wang, and F. Jin, "Robustness of China's air transport network from 1975 to 2017," *Physica A: Statistical Mechanics and its Applications*, vol. 539, article 122876, 2020.
- [23] S. R. Leonidas, D. Robert, and W. Verbeke, "A study of the U.S. domestic air transportation network—temporal evolution of network topology and robustness from 2001 to 2016," *Journal of Transportation Security*, vol. 14, no. 1-2, pp. 55–78, 2021.
- [24] L. Zhang, Y. N. Zhao, D. L. Chen, and X. H. Zhang, "Analysis of network robustness in weighted and unweighted approaches: a case study of the air transport network in the belt and road region," *Journal of Advanced Transportation*, vol. 2021, Article ID 8810254, 13 pages, 2021.
- [25] G. J. Ren, "Robustness analysis of air route network based on topology potential and relative entropy methods," *Journal of Advanced Transportation*, vol. 2021, Article ID 5527423, 11 pages, 2021.
- [26] A. Cardillo, M. Zanin, J. Gómez-Gardeñes, M. Romance, A. J. García del Amo, and S. Boccaletti, "Modeling the multi-layer nature of the European air transport network: resilience and passengers re-scheduling under random failures," *The European Physical Journal Special Topics*, vol. 215, no. 1, pp. 23–33, 2013.
- [27] T. Verma, N. A. M. Araujo, and H. J. Herrmann, "Revealing the structure of the world airline network," *Scientific Reports*, vol. 4, no. 1, p. 5638, 2014.
- [28] W. B. Du, X. L. Zhou, O. Lordan, Z. Wang, C. Zhao, and Y. B. Zhu, "Analysis of the Chinese airline network as multi-layer networks," *Transportation Research Part E*, vol. 89, pp. 108–116, 2016.
- [29] C. Hong, J. Zhang, X. B. Cao, and W. B. Du, "Structural properties of the Chinese air transportation multilayer network," *Chaos Solitons & Fractals*, vol. 86, pp. 28–34, 2016.
- [30] O. Lordan and J. M. Sallan, "Analyzing the multilevel structure of the European airport network," *Chinese Journal of Aeronautics*, vol. 30, no. 2, pp. 554–560, 2017.
- [31] L. Zhang, H. R. Du, Y. N. Zhao, P. D. Maeyer, and B. Desein, "Drawing topological properties from a multi-layered network: the case of an air transport network in "the belt and road" region," *Habitat International*, vol. 93, article 102044, 2019.
- [32] H. Zhang, H. D. Cui, W. Wang, and W. B. Song, "Properties of Chinese railway network: multilayer structures based on timetable data," *Physica A: Statistical Mechanics and Its Applications*, vol. 560, article 125184, 2020.
- [33] Y. Yang, K. J. Xu, and C. Hong, "Network dynamics on the Chinese air transportation multilayer network," *International Journal of Modern Physics C*, vol. 32, no. 5, article 2150070, 2021.
- [34] Z. Guo, M. Hao, B. Yu, and B. Z. Yao, "Detecting delay propagation in regional air transport systems using convergent cross mapping and complex network theory," *Transportation Research Part E*, vol. 157, article 102585, 2022.
- [35] F. Xie, M. Ma, and C. Ren, "Research on multilayer network structure characteristics from a higher-order model: the case of a Chinese high-speed railway system," *Physica A: Statistical Mechanics and its Applications*, vol. 586, article 126473, 2022.